High-Frequency Dynamic Nuclear Polarization NMR for Solids: Part 1 – An Introduction

57

Michelle Ha and Vladimir K. Michaelis

Contents

Introduction 1184
High-Frequency DNP NMR Instrumentation 1185
Solid-State NMR Spectrometer 1185
Microwave Devices 1185
Cryogenics 1187
DNP NMR Probe 1188
DNP Mechanisms 1189
Cross Effect DNP Mechanism 1190
Solid Effect DNP Mechanism 1191
Polarizing Agents 1192
Narrow-Line Polarizing Agents 1193
Wide-Line Polarizing Agents 1194
Sample Preparation 1196
Summary and Future Outlook 1199
References 1199

Abstract

Dynamic nuclear polarization (DNP) NMR spectroscopy, a high-polarization method, is rapidly changing the landscape of what is possible in solid-state nuclear magnetic resonance spectroscopy. To date, there have been over 200 publications discussing high-frequency DNP NMR of solids with more than half being released within the past few years. Below we provide for researchers that may be interested in this high-sensitivity technique an introduction to high-frequency DNP NMR spectroscopy, including instrumentation, mechanisms, polarizing agents, and sam-

M. Ha · V. K. Michaelis (✉)
Department of Chemistry, University of Alberta, Edmonton, AB, Canada
e-mail: michelle.ha@ualberta.ca; vladimir.michaelis@ualberta.ca

G. A. Webb (ed.), *Modern Magnetic Resonance*,
https://doi.org/10.1007/978-3-319-28388-3_140

ple preparation. While there are many applications utilizing high-frequency DNP NMR, Part II will deal with recent advances in method development and applications to biomolecular solids and materials science.

Keywords
Dynamic nuclear polarization · Nuclear magnetic resonance · Magic angle spinning · High polarization · High field · Microwave · Gyrotron · Glassing agent · Radical · Polarizing agent · Mechanism · Cryogens · High sensitivity · Instrumentation · Cross effect · Biradical · Biomolecular · Materials

Introduction

Solid-state nuclear magnetic resonance (NMR) spectroscopy is a mature field and arguably one of the most robust analytical techniques for characterizing atomic- and molecular-level structure in solids. It can be found in nearly every scientific discipline such as biomolecular, chemical, materials and earth science due to the unique ability to probe subnanometer short- and medium-range structure of ordered and disordered solids. A particular strength of NMR spectroscopy is its ability to elucidate various isotropic and anisotropic interactions that are rich in atomic- or molecular-level structural and dynamic information. For example, dipolar coupling (a through space interaction) is readily used to address medium-range order within solids [1–5]. The isotropic chemical shift is vital in identifying functional groups within organic molecules, polymorphs in pharmaceutical compounds, or coordination environments and bonding arrangements important in materials science and geoscience [6, 7]. The quadrupolar interaction, affecting over 70% of the NMR-active nuclei on the periodic table, is highly sensitive to the overall molecular and atomic environment. The magnitude and shape of the interaction has aided in studying many chemical systems [8, 9].

The large versatility of NMR spectroscopy can be overshadowed by the small nuclear Zeeman polarization resulting in poor overall sensitivity. Solids are particularly disadvantaged as many suffer from broad NMR resonances ranging between 10s of kHz (dipolar coupling, magnetic shielding) to MHz (quadrupolar coupling) and a range in relaxation properties (e.g., T_1 and T_2). Over the past 50 years, several innovations have advanced the field, providing practical gains in sensitivity. The first breakthrough was made by Andrew and Lowe [10, 11] who introduced magic-angle spinning; another important advance was the introduction of cross-polarization [12] (CP). In the early 1990s progress in high-field NMR magnets surged, with the introduction of ultrahigh-field magnets from a host of commercial and home-built systems; today commercial systems exist as high as 1 GHz, with plans for 1.2 and 1.3 GHz in the very near future [13, 14]. At each stage these developments have left a lasting impact in the field of NMR spectroscopy.

With the recent commercialization of dynamic nuclear polarization (DNP), a high-polarization technique in NMR spectroscopy, the field is undergoing a rapid change due to the technique's unprecedented sensitivity [15, 16]. DNP NMR

involves transferring the large electron polarization of unpaired electron spins to nearby insensitive nuclei via microwave irradiation of the electron-nuclear transitions, resulting in sensitivity gains in varying orders of magnitude (i.e., 10–100 [3]) over traditional NMR spectroscopy (e.g., up to 658-fold (γ_e/γ_n) increase in the case of ^{1}H). This makes otherwise impossibly long experiments practical to complete. For example, an enhancement factor (ε) of 20 reduces the required experimental time by a factor of 400 (20^2), reducing experimental times from months to hours and opening new frontiers for scientific exploration.

To gain a better understanding of the various components necessary for high-frequency DNP NMR, this article contains two parts, below (Part I) will provide an overview of the instrumentation, mechanisms, polarizing agents, and sample preparation that are commonly used within the field; Part II highlights the new areas DNP NMR is making available to the research community including DNP method development, biomolecular solids, and materials science. Many excellent reviews have emerged over the years, and the following articles are recommended for interested readers [17–28].

High-Frequency DNP NMR Instrumentation

Robust and reliable instrumentation is essential to performing experimental high-frequency DNP research and is still a key barrier in implementing DNP NMR within international research groups. A DNP NMR spectrometer (Fig. 1) is comprised of four major components: (i) a solid-state NMR spectrometer, (ii) a microwave device and accessories, (iii) cryogenics, and (iv) a DNP NMR probe.

Solid-State NMR Spectrometer

A conventional NMR spectrometer (i.e., superconducting magnet, spectrometer, pneumatic control system, user interface, etc.) is required to perform NMR experiments. For DNP NMR, the magnet bore must be 89 mm (i.e., wide-bore) rather than a standard bore of 51 mm to accommodate the probe electronics, dewar, microwave waveguide, sample eject, and insulation requirements for performing low-temperature experiments. Another consideration is whether the main magnetic field is coupled to an outer coil that can be adjusted to varying degrees (i.e., a sweep coil) to increase or decrease the field strength in fine steps. This is particularly important for radical development and for other targeted applications. The sweep coil enables one to optimize the strength of the main magnetic field for advanced applications.

Microwave Devices

One of the most challenging pieces of instrumentation to develop is a source that generates high-frequency microwaves. With high-frequency DNP NMR now

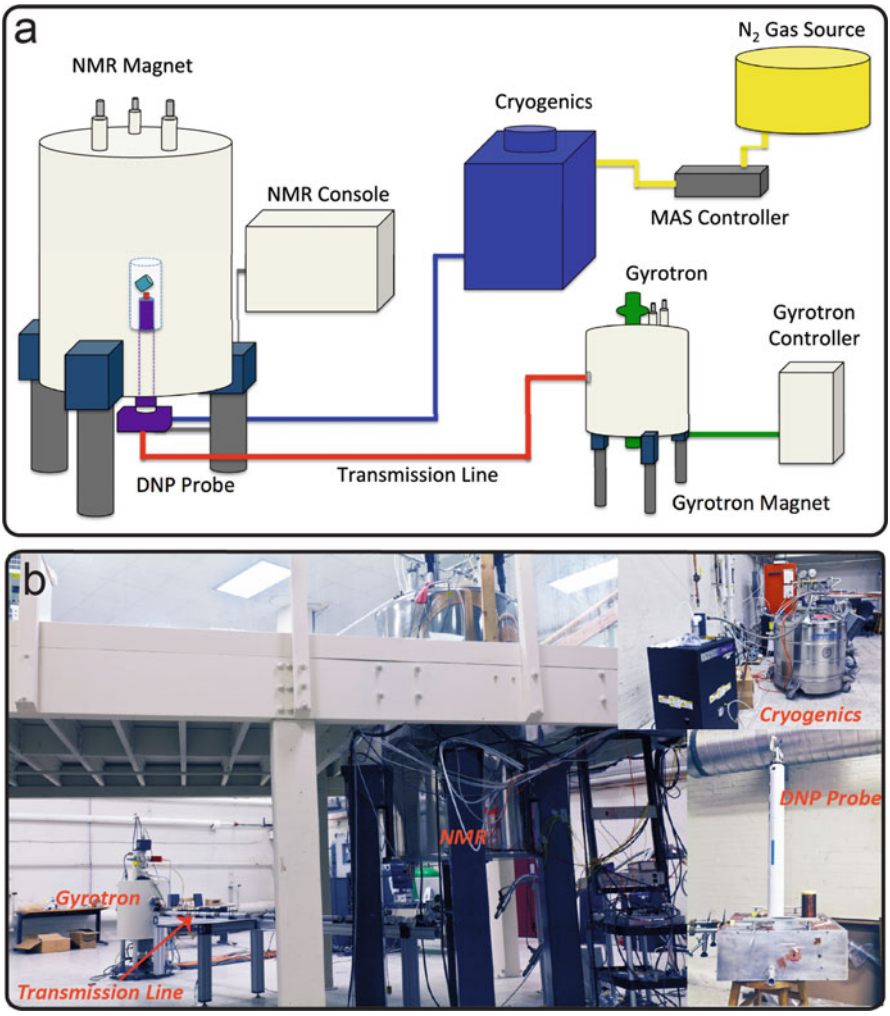

Fig. 1 (**a**) Schematic of a high-frequency DNP NMR spectrometer and (**b**) photo of a 699 MHz/460 GHz DNP NMR spectrometer (Francis Bitter Magnet Laboratory, Massachusetts Institute of Technology, Cambridge, MA, USA) including (i) solid-state NMR spectrometer, (ii) gyrotron and transmission line, (iii) cryogenics, and (iv) DNP NMR probe

ranging from 5–19 T (200–800 MHz), microwave devices must generate microwaves in the 140–527 GHz frequency range. The most commonly applied device is known as a gyrotron. This is in part due to the significant development in gyrotron technology for the application in DNP NMR carried out by Temkin and Griffin at MIT [29–33], by Osaka University and the University of Fukui [34–36] and commercially by Bruker Biospin, Communications and Power Industries (CPI), and by Bridge12.

The basis of a gyrotron is its use of stimulated cyclotron radiation generated when present in a superconducting magnet. A gyrotron is capable of generating high-power microwaves at high frequency (>100 GHz). The fast-wave device is often operated in a higher mode which improves the robustness and cooling abilities providing a microwave device that is extremely stable, with high output power and continuous operation for days to months. The design of these devices is also attractive for their longevity with lifetimes expected to be 10+ years. These features make them ideal for NMR studies where experiments often require days to weeks of continuous acquisition. As discussed above, the NMR spectrometer may be equipped with a sweep coil to allow fine adjustments of the field strength. If this is not possible, an alternative is having a tunable microwave device such as a tunable gyrotron, as one can fluctuate the output of the microwave frequency while keeping the main magnetic field of the NMR instrument constant [33, 37–40]. However, an issue to be aware of is maintaining a stable and constant microwave output over a wide tuning range.

Alternative microwave sources, optimal for applications below 5 T, including extended interaction Klystrons (EIK), oscillators (EIO), and amplifiers (EIA), have also been successfully applied to higher field strengths; for example the Tycko group has an operational system at 9.4 T (400 MHz, ^{1}H, and 264 GHz, e^{-}) [41]. Unfortunately, these alternatives suffer from limited output power at high frequencies, ~5 W at 265 GHz, which affects enhancements and strains the device, limiting their longevity (lifetimes of ~10,000 h, ~1.2 years at 265 GHz). Furthermore, commercial units are unavailable for applications above 265 GHz. As advancements and demand of microwave technology continue, these sources may be attractive for certain DNP applications as they become available at higher magnetic fields and/or microwave output powers.

Cryogenics

Conventional DNP NMR relies on the ability to cool the sample to cryogenic temperatures to improve the electron and nuclear relaxation behavior, aiding the effective transfer of bulk polarization within the sample. This can be accomplished by using a cryogenic heat exchanger whereby a sealed can within a larger container of liquid nitrogen is pressurized to provide a stream of gas at cryogenic temperatures [42]. By adjusting the pressure within the heat exchanger, one can control the output temperature. Finer control can easily be achieved using a cryogenic temperature control (e.g., Lakeshore unit) that can be equipped with a heater to regulate the output gas to within 1 K or better. Similar types of devices have been successfully implemented using liquid He although the increasing cost of He is a prominent concern. Breakthroughs in DNP have occurred with recirculated He; in particular, the groups of De Paëpe [43] and Matsuki [35] have successfully designed a closed-loop system for their DNP NMR instrument that can operate at He temperatures. Tycko et al. [44, 45] and Levitt et al. [46] have also recently contributed to the He-cooled MAS NMR area. The major expense of DNP beyond the initial investment in infrastructure is its thirst for cryogens (both N_2 and He). Hence, the authors

believe a worthwhile goal of this field as it matures should be to strive to reduce the operating costs associated with the cryogens. For example, cryogenic pre-chillers and nitrogen gas generators have been successfully used in Osaka University [36] and MIT [47].

DNP NMR Probe

The NMR probe is responsible for sending and detecting the signal during an NMR experiment, and if necessary, cooling the sample, rotating the sample, and providing the conduit for microwave irradiation prompting the transfer of polarization between electron and nuclear spins. A cryogenic DNP NMR probe is based on conventional home-built or commercial MAS NMR probes, but a few key modifications are required. The lines that provide a stream of compressed gas (i.e., drive and bearing) to levitate and rotate the rotor must be vacuum jacketed. The insulation enables the transfer of chilled gas for the drive and bearing to cool the sample and probe. Typical spinning frequencies are between 4 and 20 kHz, but newly designed commercially available probes are capable of spinning samples up to 40 kHz (depending on rotor size and experimental temperature). In the foreseeable future, frequencies >40 kHz will surely be attained as room temperature probes are capable of spinning frequencies beyond 100 kHz [48]. The stator housing requires a modification near the coil to accommodate the microwave transmission line, responsible for guiding and projecting the microwave beam onto the rotor. The probe is often encased within a vacuum jacketed dewar to aid in localized cooling of the probe, and more importantly to protect the bore of the NMR magnet (T = ~290 K) from the cryogenic temperatures (<120 K) located within the probe. Samples can be placed into zirconia or sapphire NMR rotors, the latter appear to provide larger enhancements, although thin-wall zirconia is proving quite successful commercially and is slightly more robust. The drive caps can be Torlon® or Vespel® that are glued using cryo-epoxy or machined zirconia in combination with a small polymer plug.

It should be noted that several variations from this general design model do exist. A few noteworthy differences include: (i) an added variable temperature line (3rd vacuum jacketed line) that can accommodate N_2 or He to assist in cooling, [44, 47] (ii) the microwave waveguide may be directed at the top of the stator or pointed to the head of the NMR rotor, [36] (iii) sample ejection [47, 49, 50] for ease of changing samples (above or below models exist), and (iv) the gyrotron may be placed above the probe using the same superconducting magnet to produce microwaves and record the NMR experiment. As the probe body is cooled, this does affect the overall behavior of the electronics which can have positive benefits in generating high RF fields (i.e., $\gamma B_1/2\pi$), but it can also affect the tuning circuit. In regards to the RF design, the most effective approach has been a topic of discussion for many years, issues include whether the probe design should be transmission line versus locally tuned and weighing the benefits of implementing a balanced RF circuit design [44, 45, 51–58].

Table 1 Examples of homebuilt and commercial DNP NMR instruments

Type	Location/ manufacturer	B_o (MHz/GHz)	Microwave source	Completed
Home-built	MIT	211/140 [30, 59] 380/250 [29, 38, 60] 700/460 [23, 33, 47] 500/330 [32, 39] 800/527 [31]	Gyrotron Gyrotron Gyrotron Gyrotron Gyrotron	*ca.* 1991–1993 *ca.* 2002–2003 *ca.* 2011–2013 *ca.* 2014–2016 *in-prep.*
Home-built	NIH	400/263 [41]	Diode	*ca.* 2009–2010
Home-built	Osaka	600/395 [36, 40] 700/460 [34, 35]	Gyrotron Gyrotron	*ca.* 2010–2012 *ca.* 2015–2016
Home-built	Warwick	284/187 – 600/395 [61]	Gyrotron	*ca.* 2012
Home-Built	Washington U. St. Louis	300/198 [62]	Gyrotron	*ca.* 2016–2017
Commercial	Bruker Biospin [48, 50]	400/263 600/395 800/527	Gyrotron Gyrotron Gyrotron	*ca.* 2009–2010 *ca.* 2011–2012 *ca.* 2012–2013

As the field has rapidly advanced with the introduction of commercial units in 2010, systems have been successfully implemented in several research groups worldwide; a few are summarized in Table 1.

DNP Mechanisms

For solids using a continuous microwave source there are four DNP mechanisms that can be considered in order to achieve bulk polarization transfer between an unpaired electron source (polarizing agent) and a nucleus: (i) thermal mixing (TM), (ii) Overhauser effect (OE), (iii) solid effect (SE), and (iv) cross effect (CE). The latter mechanism is by far the most targeted area in high-frequency DNP NMR applications due to the wide array of wide-line nitroxide radicals that favor the polarization of high-gamma nuclei (i.e., ^{1}H). SE has been effective at lower field strengths [63] although a range of developments and results have recently appeared in the literature [64–66] so that it is still an active field of study in high-frequency DNP development. Likewise, Overhauser effect has recently emerged as a contender for higher field DNP NMR [67, 68]. Further developments with radicals could be fruitful as the enhancements scale linearly with magnetic field strength. Below is a

brief overview of the CE and SE DNP mechanisms; the following references are provided for a more comprehensive review [15, 16, 21, 24, 27, 65, 67–83].

The dominant DNP mechanism depends on the targeted NMR-active nucleus and on the EPR characteristics of the selected polarizing agent. For example, the most common approach in DNP NMR applications of solids is through indirect polarization transfer using a CP step ($e^- \rightarrow {}^1H \rightarrow X$, where X is a lower gamma nucleus). Using this approach one can select for SE by using a narrow-line radical such as trityl or for CE with TOTAPOL, a wide-line biradical. In other words, it is the relative magnitudes of the electron homogeneous (δ) and inhomogeneous (Δ) linewidths, and the nuclear Larmor frequency (ω_{0I}) that guide the DNP mechanism.

Cross Effect DNP Mechanism

The CE mechanism can be described as a three-spin flip-flop-flip process between two electrons and a nucleus, which is dominant when $\Delta > \omega_{0I} > \delta$. The difference between the two electron Larmor frequencies should be near the nuclear Larmor frequency to achieve maximum polarization transfer between electron and nuclear spins [73, 75, 79, 84].

$$\omega_{0I} = \omega_{0S_2} - \omega_{0S_1} \tag{1}$$

To satisfy Eq. 1 for high-gamma nuclei like ^1H, the polarizing agent needs to have EPR characteristics (EPR spectrum) of a broadline; this is readily seen in nitroxide-based radicals including monoradicals such as TEMPO and TEMPONE, and biradicals such as SPIROPOL, AMUPOL, and TEKPOL. The need to have two electrons in close proximity (i.e., dipolar coupled) while minimizing the paramagnetic bleaching of nuclear spins has pushed the field into biradicals [85, 86]. Tethered radicals provide the chemical design to reasonably direct orientation and electron-electron distance so that the dipolar coupling is on the order of 20–35 MHz, while enabling the concentration of unpaired electrons to be minimized, typically $<$15 mM solution (i.e., $<$30 mM electrons). In contrast to biradicals, monoradicals with a 40 mM electron concentration have significantly reduced dipolar couplings of $<$2 MHz when present in a homogenous glassy sample [85–88]. The CE mechanism is often the choice for high-frequency DNP NMR experiments as the mechanism is based on allowable transitions (Fig. 2) and loosely scales with the inverse of magnetic field strength. In the past few years, descriptions of the CE mechanism taking into account the level crossing that occurs under magic-angle spinning has shed further light into the spinning rate dependence of the overall enhancement. The reader is referred to the works by the Tycko [89] and Vega [81] groups where they discuss modulations of the energy levels within DNP mechanisms when using magic-angle spinning and the impact it has on polarization transfer.

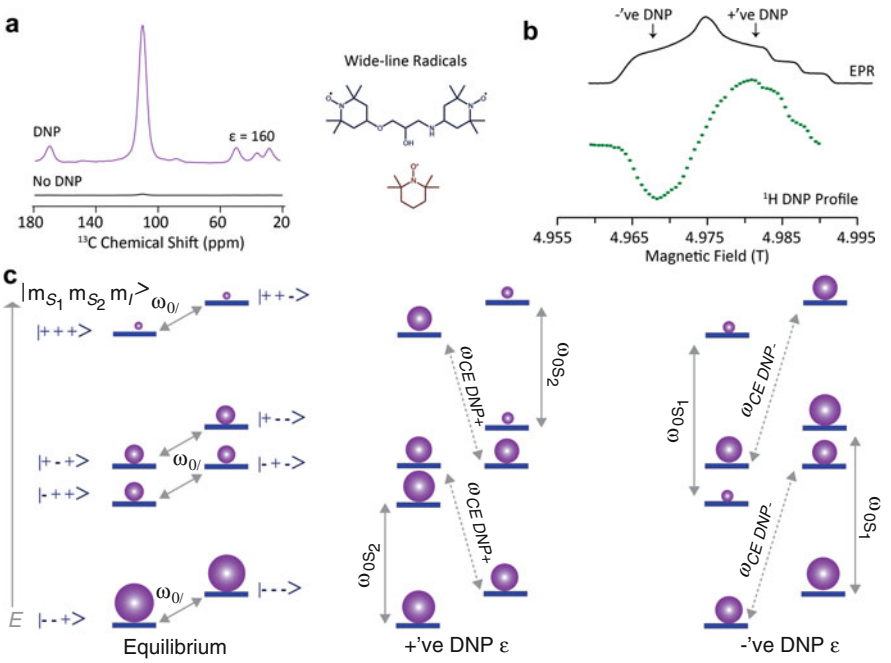

Fig. 2 Cross effect DNP: (**a**) on (DNP) and off (No DNP) $^{13}C[^{1}H]$ CP MAS NMR experiment on urea using a wide-line nitroxide radical, (**b**) EPR and ^{1}H DNP NMR field profile for a nitroxide polarizing agent, and (**c**) energy level diagram for CE DNP displaying spin population distribution for a three-spin (two electrons and one nucleus) system at thermal equilibrium, positive and negative CE DNP conditions. Microwave saturation of the electron transition (ω_{0S1} or ω_{0S2}) leads to a three-spin flip-flop-flip process that distributes the population (ω_{CE}), thus increasing the net nuclear polarization

Solid Effect DNP Mechanism

The SE mechanism can be described as a two-spin process involving an electron and a nucleus. The SE mechanism is dominant when the nuclear Larmor frequency is larger than the electron homogeneous and inhomogeneous EPR linewidths ($\omega_{0I} > \delta, \Delta$), and microwave irradiation is applied at the electron-nuclear zero- or double-quantum transition as shown in Fig. 3 [65, 66, 69, 90]. The SE matching condition is satisfied when:

$$\omega_{mw} = \omega_{0S} \pm \omega_{0I} \tag{2}$$

where ω_{0S} and ω_{mw} are the electron Larmor and microwave frequencies, respectively. The mechanism may be observed when a narrow-line radical (e.g., BDPA, trityl, etc.) is used as the polarizing agent (narrow EPR spectrum) and has an electron spin-lattice relaxation time (T_{1S}) that is optimized to allow for efficient polarization transfer to nearby NMR-active nuclei.

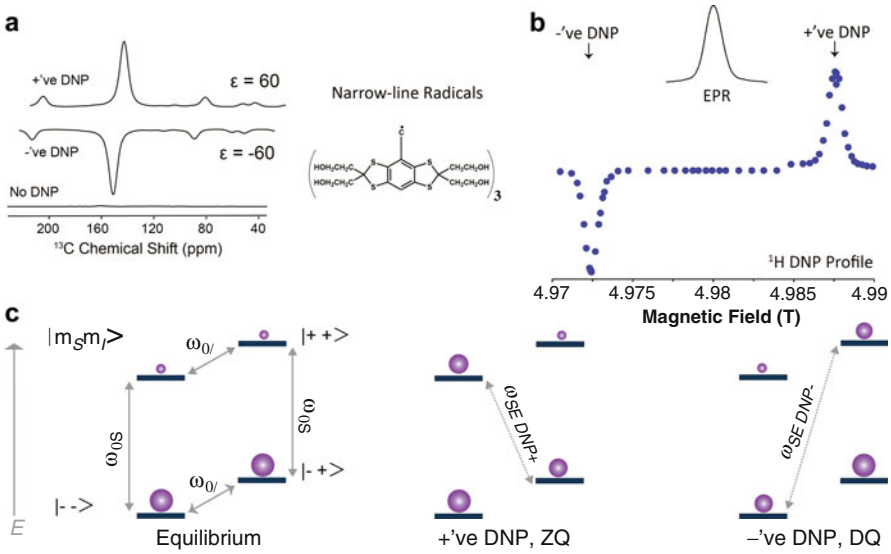

Fig. 3 Solid effect DNP: (**a**) on (DNP) and off (No DNP) experiment showing the positive and negative DNP enhancement ($^{13}C[^{1}H]$ CP MAS NMR experiment on urea using a narrow-line radical), (**b**) EPR and ^{1}H DNP NMR field profile for a narrow-line polarizing agent, and (**c**) energy level diagram for SE displaying spin-population distribution for a two-spin (one electron and one nucleus) system at thermal equilibrium, positive ($\omega_{0S} - \omega_{0I}$, ZQ) and negative, ($\omega_{0S} + \omega_{0I}$, DQ) DNP enhancements

Polarizing Agents

Dynamic nuclear polarization requires a source of unpaired electron spins, which is typically achieved using exogenous organic-based radicals also known as polarizing agents. Radicals are typically divided into two categories as either narrow-line or wide-line radicals based on their EPR characteristics, since it is the EPR characteristics of the polarizing agent that give insight into what type of DNP mechanism governs the $e^- - n^o$ polarization transfer. For several compelling reasons, including its reduced spin−lattice relaxation, improved sensitivity possible through CP, and a large database of nitroxide radicals, ^{1}H is often the nucleus of choice for initial polarization at cryogenic temperatures using a wide-line biradical polarizing agent. Subsequent to polarization of ^{1}H, a CP step is used to observe low-gamma nuclei. This indirect polarization transfer method ($e^- \rightarrow {}^{1}H \rightarrow X$, Fig. 4) has been successfully applied to a wide range of solids including biomolecular, materials and surfaces [18–20, 91]. An alternative to indirect polarization is polarizing an NMR active nucleus (X) directly from a source of unpaired electrons, $e^- \rightarrow X$ (i.e., direct polarization, Fig. 4) [23, 87, 88, 92–95]. This approach is of interest for many chemical systems that do not cross-polarize efficiently by high-γ nuclei (e.g., ^{1}H or ^{19}F), or those where the high-γ nuclei are absent, and the approach may be of

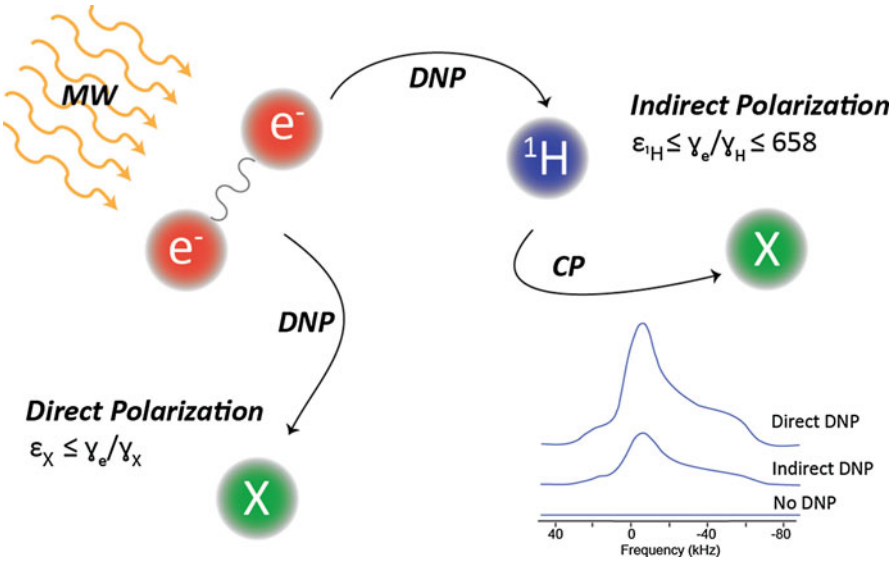

Fig. 4 Schematic of indirect (through ^{1}H's) and direct e^{-} – n^{o} polarization transfer pathways in DNP NMR of solids. Indirect polarization (most common) enhances ^{1}H (ε_{1H}), with a theoretical gain in sensitivity of 658, which can then be transferred to NMR-active nuclei of interest such as ^{13}C, ^{15}N, ^{17}O, etc. Direct polarization (less common) enhances NMR active low-gamma nuclei directly (not through a cross-polarization step from ^{1}H or ^{19}F). The theoretical gain depends on the NMR active nucleus, such as 2,618 for ^{13}C (ε_{13C}), 3,311 for ^{29}Si (ε_{29Si}), 4,855 for ^{17}O (ε_{17O}), 6,493 for ^{15}N (ε_{15N}), etc.

assistance in spectral editing to distinguish between protonated and nonprotonated chemical environments.

The choices can be vast as many organic radicals exist, particularly with the recent explosive developments in high-frequency DNP NMR and the push for improved biradicals. Below, we highlight a few of the key polarizing agents that are often used for various applications, organized by their characteristic EPR spectra of narrow-line and wide-line radicals.

Narrow-Line Polarizing Agents

Within the DNP NMR field, only a handful of narrow-line radicals are currently viable. Although limited in options, these chemically designed radicals provide an interesting array of tunability allowing the selection of different DNP mechanisms and permitting an exploration into various direct and indirect polarization methods. Generally, these narrow-line radicals have been used within applied fields (*vide infra*), and can display the CE or SE DNP mechanism depending on the NMR-active nucleus being probed. In the case of ^{1}H, these radicals exhibit solid-effect characteristics which scale unfavorably with field strength dependence

($\varepsilon \propto {B_0}^{-2}$) [96]. This may change as microwave technology emerges offering higher-output power able to circumvent the losses from increased B_0.

Figure 5 illustrates a series of narrow-line radicals that have been successfully applied to various chemical problems. They are promising candidates for low-gamma polarization including ^{13}C [88, 94, 97], ^{2}H [93], ^{17}O [23, 87], and ^{29}Si [98], as these begin to satisfy the CE DNP mechanism of low-gamma nuclei via direct polarization. This may be attractive for materials that do not contain high-gamma nuclei or solids that suffer from extremely long ^{1}H T_1's. Recently, research has begun to emerge adopting the Overhauser DNP mechanism for ^{1}H at high magnetic fields using narrow-line radicals [67, 68, 99]. As the Overhauser effect is the only DNP mechanism that improves with magnetic field strength and requires little microwave power to saturate the electrons [99], it may offer significant advantages including permitting the use of low-power microwave sources (e.g., EIK). As the field turns to higher and higher magnetic fields (>800 MHz), alternative radicals will surely be developed.

Wide-Line Polarizing Agents

The most prominent radicals used in DNP NMR applications are wide-line polarizing agents, typically comprised of nitroxide moieties. These are chosen due to the range of offerings within the literature and/or commercial sources, synthetic tunability, and ease in which they satisfy the CE DNP mechanism for ^{1}H. In most applications of DNP NMR, polarization transfer occurs indirectly through high-polarized protons and a CP step to lower gamma nuclei such as ^{13}C, ^{15}N, or ^{29}Si. As outlined above, targeting ^{1}H is advantageous; in addition, in some cases this approach allows one to tune the ^{1}H spin-lattice relaxation and ^{1}H-^{1}H spin-diffusion behavior through ^{2}H exchange (i.e., adjusting the ^{1}H to ^{2}H ratios within the solvent and/or solid of interest).

Early work focused on monoradicals, typically involving TEMPO-based derivatives which are easily sourced. To reach maximum CE DNP enhancements, quantities of 40+ mM electrons were required as at this level favorable $e^- - e^-$ dipole interactions on the order of a few MHz were obtained, but this caused significant paramagnetic relaxation resulting in a loss of signal as well as reduction in T_2, affecting resolution. In 2006, Song and Hu, graduate students within the Swager and Griffin groups (MIT), respectively, synthesized a highly effective and water soluble biradical known today as TOTAPOL [86]. This began the movement to utilize biradicals which permit a reduction of the concentration of the polarizing source (5–15 mM biradical or 10–30 mM electrons) and consequently reduce signal quenching [100] while yielding larger enhancements as the two electrons required within the three-spin CE DNP mechanism are highly coupled due to the chemical tether. Current research suggests that a dipolar coupling of between 25 and 35 MHz, the relative orientation between the two organic radical moieties and the exchange interaction appear to be important factors [96, 101–103].

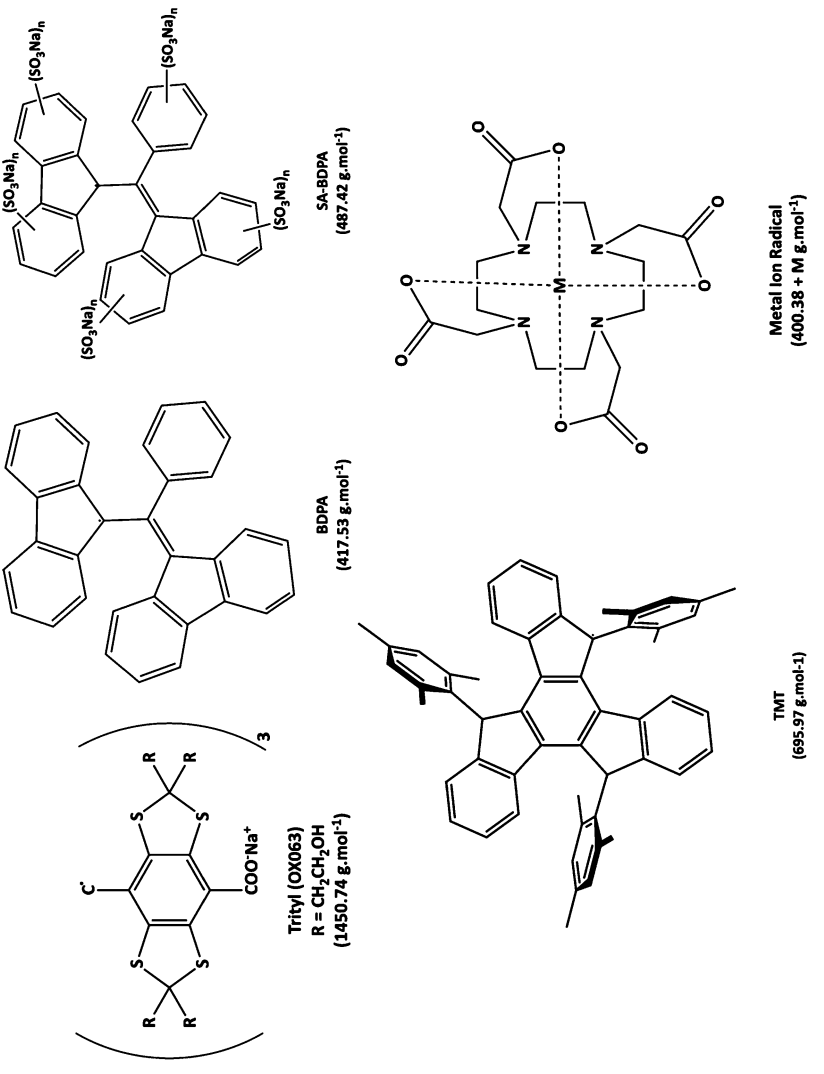

Fig. 5 Common narrow-line radicals used as polarizing agents in high-frequency DNP NMR

For years two biradicals, bTbK [104] and TOTAPOL [86] (Fig. 6), were the benchmarks for high-frequency DNP, but with the introduction of commercial instrumentation, advances in both organic and water soluble radicals has exploded since 2013. The nature of biradicals have varied using a host of species; some of the most efficient radicals that have emerged include AMUPOL (hydrophilic biradical) [105] and TEKPOL derivatives (hydrophobic biradical) [103, 106], among many others [86, 102, 104–111].

Emerging areas in radical development include a report highlighting the benefit of using a mixed biradical that tethers a TEMPO and trityl moiety. The report demonstrates the excellent high-field enhancements, surpassing conventional biradical nitroxides as well as reducing the signal quenching of the sample, adding another dimension worth exploring in this exciting field [101]. There have also been advances in the use of paramagnetic metals as DNP polarizing agents including homogeneous solids, biomolecular and inorganic chemical systems [64, 112–115]. There is no doubt that radical development will continue to advance along with high-frequency DNP.

Sample Preparation

The vast majority of high-frequency DNP NMR experiments applied to chemical systems utilize an ex situ polarizing agent with a cryoprotectant. A DNP sample will consist of a polarizing agent, typically a biradical in 10 ± 5 mM concentration, a solvent mixture and the sample of interest. The cryoprotectant (i.e., solvent mixture) is important for several reasons such as allowing the homogeneous dispersion of the polarizing agent within the sample, assisting in providing uniform polarization across the sample and protecting the sample from cryogenic temperatures (particularly important in biological specimens). When choosing a solvent mixture one should consider whether the solvent is more likely to have an amorphous-like consistency or to crystallize, as this has drastic effects on the enhancement efficiency as well as on radical homogeneity [109]. It is also important to ensure the solvent does not react with the sample of interest. Typically, a glycerol-water (60:40, v/v) mixture is the most effective solvent, forming an excellent glass at cryogenic temperatures. Glycerol has been used for decades as a cryoprotecting medium in a host of research projects requiring low-temperature experiments. Other solvent mixtures that appear in the DNP literature include DMSO/water (60:40, v/v), dichloroethane/methanol (95:5, v/v), o-terphenyl, etc. [23, 50, 109, 116–120] Typically, hydrophilic solvents are preferred for biomolecular solids while hydrophobic solvents are preferred for inorganic solids.

One further step in choosing the appropriate solvent mixture is the ability to exchange isotopes. In general, a ^{1}H concentration of approximately 10% within a solvent has been found to be an effective ^{1}H spin-bath reservoir. Thus, for example, the ^{1}H concentration in the glycerol/water mixture (colloquially referred to as *DNP Juice*) is diluted to approximately 10% using a combination of glycerol-d_8, D_2O, and H_2O (60:30:10, v/v/v).

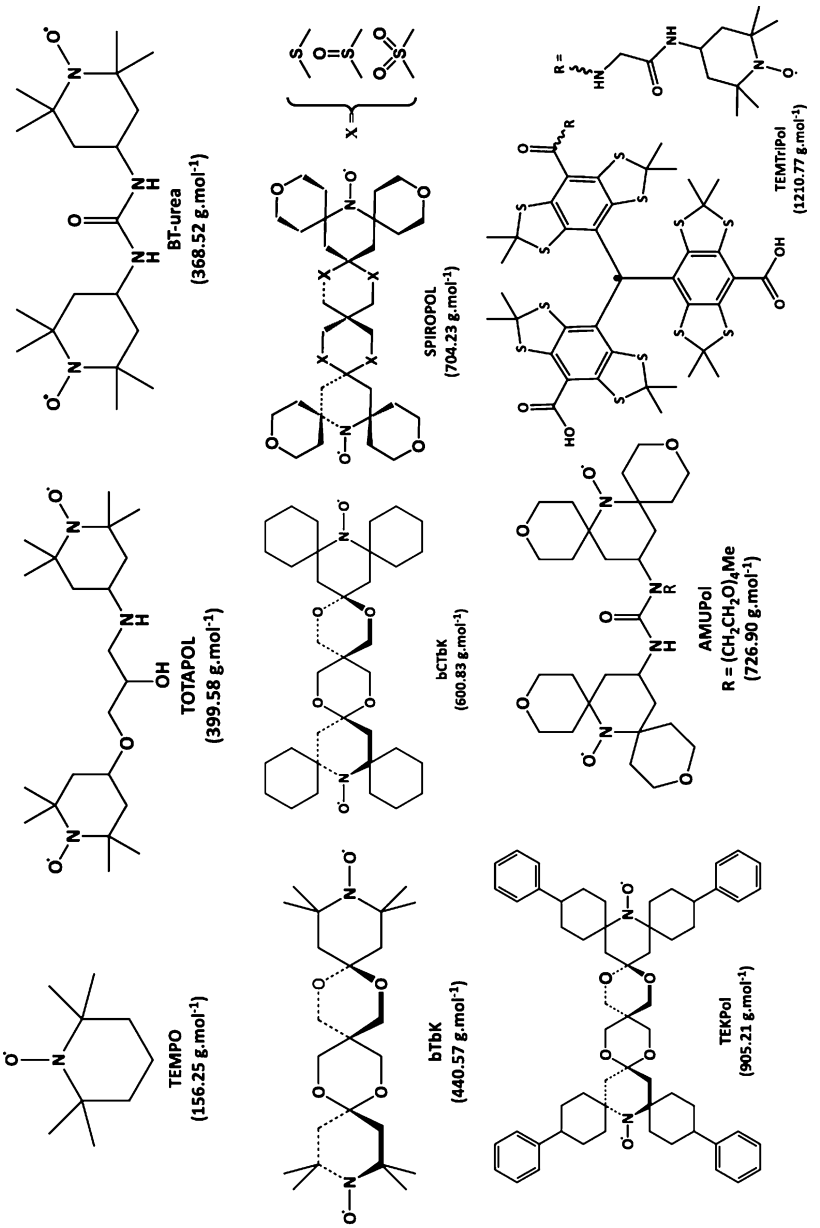

Fig. 6 Common wide-line radicals used as polarizing agents in high-frequency DNP NMR

A homogenous sample is one where the radical and chemical sample is readily dissolved in the solvent-matrix and upon quenching a homogeneous glass is formed. This approach often leads to the most effective polarization transfer as the radical is effectively distributed throughout the sample. DNP NMR of a homogeneous, amorphous chemical system can be limited in resolution due to line-broadening stemming from a distribution of chemical shifts, a commonly observed occurrence for many organic and inorganic amorphous materials, as well as from slower side-chain dynamics at cryogenic temperatures. A heterogeneous sample is one where the solvent matrix (radical and solvent) are in contact with the chemical sample, although the sample of interest does not readily dissolve in the matrix. Large enhancements are achievable for these systems although they are typically reduced due to inhomogeneous radical distribution, solvent selection, glassing ability, domain size, pore size, radical-sample interaction, and the limitations in effective $e^- - {}^1H$ and ${}^1H - {}^1H$ spin-diffusion across the solid [23, 66, 83, 121–126]. Dynamics and hydrogen concentrations within the sample can also affect the recorded enhancement. An added benefit of heterogeneous DNP within nano- and microcrystalline solids is that resolution is typically unhampered at cryogenic temperatures enabling both a savings in acquisition time as well as high-resolution spectra that provide detailed structural information. It has also been our experience that using low radical concentrations ($<$10 mM biradical) tends to diminish the quenching effect on spin-spin relaxation (T_2), providing higher resolution spectra, although the enhancement is reduced (a trade-off between sensitivity gain and spectral resolution). DNP NMR spectroscopy has been successfully applied to a diverse range of homogeneous and heterogeneous biomolecular [18, 29, 121, 123, 127–139] and inorganic [18, 20, 23, 121, 123, 125, 126, 140, 141] solids.

Other sample preparations have also proven effective for high-frequency DNP NMR including ones that are cryoprotectant-free, an approach that does not need a solvent, or instead one that disperses the radical with a solvent that is subsequently removed. For example, a radical that is introduced onto or into a chemical system such as cellulose or a porous material then followed by evaporation has recently shown promise for natural-abundance systems [142–144]. A self-cryoprotecting solvent-free approach using in situ or ex situ sedimented (SED) DNP within an apoferritin complex (480 kDa) and BSA has recently been described [23, 145, 146].

Although these methods lead to a more heterogeneous distribution of radicals and hence polarization is not uniform within the samples, they maintain excellent sensitivity and produce excellent spectral resolution from an overall smaller effect from paramagnetic broadening. More recently a series of in situ methods have appeared using either paramagnetic metals within inorganic solids [115] or tagging organic radicals [147] or metals [112, 114] onto biomolecular solids. These unique approaches to chemically engineering the polarizing agent within the system are interesting avenues that could improve homogenous radical dispersion within the host material, such as crystalline solids (for example, alleviate domain size issues in solids) or incorporating radicals as synthetic tags with proteins (for example, incorporating the radical in the lipid within membrane proteins, or using alternative labeling procedures to tag the protein itself).

Summary and Future Outlook

High-frequency DNP NMR will continue to revolutionize our ability to explore the most challenging spectroscopic questions. The balance between radical concentration and resolution is a critical concept that must be carefully evaluated while sample preparation is critical to one's ability to obtain the highest quality spectra. Due to the access of biradicals, glass forming solvents and ease in implementing CE DNP NMR, this area will surely lead in future DNP NMR applications and development for solids. To circumvent some of the enhancement issues at high fields and/or access to high power microwave sources, mixed and narrow-line radical development will surely continue, with the latter turning the attention to Overhauser DNP NMR.

As for the next technological challenges we face, DNP NMR growth will continue with development beyond 800 MHz/527 GHz on the horizon, faster magic-angle spinning (i.e., >40 kHz), reducing the cryogen-usage footprint and method development (e.g., electron decoupling, pulsed versus CW DNP NMR, frequency tunable microwave devices, etc.) to improve the sensitivity gains and resolution at higher magnetic fields and/or temperatures. One can foresee the day where a DNP NMR spectrometer will be as routine in research facilities as liquids and solid-state NMR spectrometers are today.

Acknowledgments VKM acknowledges the Natural Sciences and Engineering Research Council of Canada (NSERC) Discovery Grants program and the University of Alberta for funding. MH is partially supported by the Government of Alberta Queen Elizabeth II Graduate Scholarship.

References

1. Gullion T, Schaefer J. Rotational-echo double-resonance NMR. J Magn Reson. 1989;81:196.
2. Chan JC, Eckert H. Dipolar coupling information in multispin systems: application of a compensated REDOR NMR approach to inorganic phosphates rotational echo double resonance. J Magn Reson. 2000;147:170–8.
3. Daviso E, Eddy MT, Andreas LB, Griffin RG, Herzfeld J. Efficient resonance assignment of proteins in MAS NMR by simultaneous intra- and inter-residue 3D correlation spectroscopy. J Biomol NMR. 2013;55:257–65.
4. Weingarth M, Baldus M. Advances in biological solid-state NMR: proteins and membrane-active peptides. RSC; 2014. p. 1–17. Ch. 1.
5. Eckert H, Elbers S, Epping JD, Janssen M, Kalwei M, Strojek W, Voight U. Topics in current chemistry. Berlin/Heidelberg: Springer; 2004. p. 195–233.
6. MacKenzie KJD, Smith ME. Multinuclear solid-state NMR of inorganic materials. Pergamon; 2002.
7. Pretsch E, Bühlmann P, Badertscher M. Structure determination of organic compounds. Berlin/Heidelberg: Springer; 2009.
8. Wasylishen RE, Askbrook SE, Wimperis S. NMR of quadrupolar nuclei in solid materials. Wiley; 2012.
9. Kentgens APM. A practical guide to solid-state NMR of half-integer quadrupolar nuclei with some applications to disordered systems. Geoderma. 1997;80:271–306.
10. Andrew ER, Bradbury A, Eades RG. Nuclear magnetic resonnace spectra from a crystal rotated at high speed. Nature. 1958;182:1659.
11. Lowe IJ. Free induction decays of rotating solids. Phys Rev Lett. 1959;2:285–7.

12. Pines A, Gibby MG, Waugh JS. Proton enhanced NMR of dilute spins in solids. Chem Phys Lett. 1972;15:373.
13. Bascunan J, Hahn S, Park DK, Iwasa Y. A 1.3-GHz LTS/HTS NMR magnet-A Progress Report. IEEE Trans Appl Supercond. 2011;21:2092–5.
14. Bruker Biospin Bruker announces five ultra-high field NMR orders from Europe and Brazil, http://ir.bruker.com/investors/press-releases/press-release-details/2015/Bruker-Announces-Five-Ultra-High-Field-NMR-Orders-from-Europe-and-Brazil/default.aspx. Accessed 1.
15. Goldman M. Spin temperature and nuclear magnetic resonance in solids. Oxford: Clarendon Press; 1970.
16. Abragam A, Goldman M. Principles of dynamic nuclear polarization. Rep Prog Phys. 1976;41:395–467.
17. Barnes AB, De Paepe G, Van der Wel PCA, Hu K-N, Joo C-G, Bajaj VS, Mak- Jurkauskas ML, Sirigiri JR, Herzfeld J, Temkin RJ, Griffin RG. High field dynamic nuclear polarization for solid and solution biological NMR. Appl Magn Reson. 2008;34:237–63.
18. Ni QZ, Daviso E, Cana TV, Markhasin E, Jawla SK, Temkin RJ, Herzfeld J, Griffin RG. High frequency dynamic nuclear polarization. Acc Chem Res. 2013;46:1933–41.
19. Maly T, Debelouchina GT, Bajaj VS, Hu KN, Joo CG, Mak-Jurkauskas ML, Sirigiri JR, Van der Wel PCA, Herzfeld J, Temkin RJ, Griffin RG. Dynamic nuclear polarization at high magnetic fields. J Chem Phys. 2008;128:052211.
20. Rossini AJ, Zagdoun A, Lelli M, Lesage A, Copéret C, Emsley L. Dynamic nuclear polarization surface enhanced NMR spectroscopy. Acc Chem Res. 2013;46:1942–51.
21. Wind RA, Duijvestijn MJ, Vanderlugt C, Manenschijn A, Vriend J. Applications of dynamic nuclear-polarization in C-13 NMR in solids. Prog Nucl Magn Reson Spectrosc. 1985;17:33–67.
22. Su Y, Andreas L, Griffin RG. Magic angle spinning NMR of proteins: high-frequency dynamic nuclear polarization and ^{1}H detection. Annu Rev Biochem. 2015;84:465–97.
23. Michaelis VK, Ong T-C, Kiesewetter MK, Frantz DK, Walish JJ, Ravera E, Luchinat C, Swager TM, Griffin RG. Topical developments in high-field dynamic nuclear polarization. IsrJ Chem. 2014;54:207–21.
24. Atsarkin VA. Dynamic polarization of nuclei in solid dielectrics. Spv Phys Usp. 1978;21:725.
25. Abragam A, Goldman M. Nuclear magnetism: order and disorder. Oxford: Clarendon Press; 1982.
26. Mak-Jurkauskas ML, Griffin RG., High-frequency dynamic nuclear polarization. eMagRes. 2007.
27. Jeffries CD. Dynamic nuclear orientation. Interscience Publishers; 1963.
28. Ong TC, Verel R, Copéret C. In: Tranter GE, Koppenaal DW, editors. Encyclopedia of spectroscopy and spectrometry. 3rd ed. Oxford: Academic; 2017. p. 121–7.
29. Bajaj VS, Hornstein MK, Kreischer KE, Sirigiri JR, Woskov PP, Mak-Jurkauskas ML, Herzfeld J, Temkin RJ, Griffin RG. 250 GHz CW gyrotron oscillator for dynamic nuclear polarization in biological solid state NMR. J Magn Reson. 2007;189:251–79.
30. Gerfen GJ, Becerra LR, Hall DA, Griffin RG, Temkin RJ, Singel DJ. High-frequency (140 GHz) dynamic nuclear-polarization – polarization transfer to a solute in frozen aqueous-solution. J Chem Phys. 1995;102:9494–7.
31. Jawla S, Nanni E, Shapiro M, Mastovsky I, Guss W, Temkin R, Griffin R. Design of a 527 GHz gyrotron for DNP-NMR spectroscopy. 36th International Conference on Infrared, Millimeter, and Terahertz Waves (IRMMW-THz); 2011.
32. Jawla S, Reese M, George C, Yang C, Shapiro M, Griffin R, Temkin R. 330 GHz/500 MHz dynamic nuclear polarization-NMR spectrometer. IEEE International Vacuum Electronics Conference; 2016.
33. Torrezan AC, Han S-T, Mastovsky I, Shapiro MA, Sirigiri JR, Temkin RJ, Barnes AB, Griffin RG. Continuous-wave operation of a frequency tunable 460 GHz second-harmonic gyrotron for enhanced nuclear magnetic resonance. IEEE Trans Plasma Sci. 2010;38:1150–9.
34. Idehara T, Tatematsu Y, Yamaguchi Y, Khutoryan EM, Kuleshov AN, Ueda K, Matsuki Y, Fujiwara T. The development of 460 GHz gyrotrons for 700 MHz DNP-NMR spectroscopy. J Infrared Millimeter Terahertz Waves. 2015;36:613–27.

35. Matsuki Y, Idehara T, Fukazawa J, Fujiwara T. Advanced instrumentation for DNP-enhanced MAS NMR for higher magnetic fields and lower temperatures. J Magn Reson. 2016;264:107–15.
36. Matsuki Y, Takahashi H, Ueda K, Idehara T, Ogawa I, Toda M, Akutsu H, Fujiwara T. Dynamic nuclear polarization experiments at 14.1 T for solid-state NMR. Phys Chem Chem Phys. 2010;12:5799–803.
37. Barnes AB, Nanni EA, Herzfeld J, Griffin RG, Temkin RJ. A 250 GHz gyrotron with a 3 GHz tuning bandwidth for dynamic nuclear polarization. J Magn Reson. 2012;221:147–53.
38. Jawla S, Ni QZ, Barnes A, Guss W, Daviso E, Herzfeld J, Griffin R, Temkin R. Continuously tunable 250 GHz gyrotron with a double disk window for DNP-NMR spectroscopy. Journal of Infrared, Millimeter, and Terahertz Waves. 2013;34:42–52.
39. Torrezan AC, Shapiro MA, Sirigiri JR, Temkin RJ, Griffin RG. Operation of a continuously frequency-tunable second-harmonic CW 330-GHz gyrotron for dynamic nuclear polarization. IEEE Trans Electron Devices. 2011;58:2777–83.
40. Ikeda R, Idehara T, Ogawa I, Tatematsu Y, Chang TH, Chen NC, Matsuki Y, Ueda K. Fujiwara T. Development of a continuously frequency tunable gyrotron operating at the fundamental resonance for 600 MHz DNP-NMR spectroscopy. 37th International Confernce on Infrared, Millimeter, and Terahertz Waves (IRMMW-THz); 2012.
41. Thurber KR, Yau W-M, Tycko R. Low-temperature dynamic nuclear polarization at 9.4 T with a 30 mW microwave source. J Magn Reson. 2010;204:303–13.
42. Allen PJ, Creuzet F, De Groot HJM, Griffin RG. Apparatus for low-temperature magic-angle spinning NMR. J Magn Reson (1969). 1991;92:614–7.
43. Bouleau E, Saint-Bonnet P, Mentink-Vigier F, Takahashi H, Jacquot JF, Bardet M, Aussenac F, Purea A, Engelke F, Hediger S, Lee D, De Paëpe G. Pushing NMR sensitivity limits using dynamic nuclear polarization with closed-loop cryogenic helium sample spinning. Chem Sci. 2015;6:6806–12.
44. Thurber K, Tycko R. Low-temperature dynamic nuclear polarization with helium-cooled samples and nitrogen-driven magic-angle spinning. J Magn Reson. 2016;264:99–106.
45. Tycko R. NMR at low and ultralow temperatures. Acc Chem Res. 2013;46:1923–32.
46. Concistre M, Johannessen OG, Carignani E, Geppi M, Levitt MH. Magic-angle spinning NMR of cold samples. Acc Chem Res. 2013;46:1914–22.
47. Barnes AB, Markhasin E, Daviso E, Michaelis VK, Nanni EA, Jawla SK, Mena EL, DeRocher R, Thakkar A, Woskov PP, Herzfeld J, Temkin RJ, Griffin RG. Dynamic nuclear polarization at 700 MHz/460 GHz. J Magn Reson. 2012;224:1–7.
48. Rosay M, Blank M, Engelke F. Instrumentation for solid-state dynamic nuclear polarization with magic angle spinning NMR. J Magn Reson. 2016;264:88–98.
49. Barnes AB, Mak-Jurkauskas ML, Matsuki Y, Bajaj VS, van der Wel PCA, DeRocher R, Bryant J, Sirigiri JR, Temkin RJ, Lugtenburg J, Herzfeld J, Griffin RG. Cryogenic sample exchange NMR probe for magic angle spinning dynamic nuclear polarization. J Magn Reson. 2009;198:261–70.
50. Rosay M, Tometich L, Pawsey S, Bader R, Schauwecker R, Blank M, Borchard PM, Cauffman SR, Felch KL, Weber RT, Temkin RJ, Griffin RG, Maas WE. Solid-state dynamic nuclear polarization at 263 GHz: Spectrometer design and experimental results. Phys Chem Chem Phys. 2010;12:5850–60.
51. Markhasin E, Hu J, Su Y, Herzfeld J, Griffin RG. Efficient, balanced, transmission line RF circuits by back propagation of common impedance nodes. J Magn Reson. 2013;231:32–8.
52. Gor'kov PK, Brey WW, Long JR. Probe development for biosolids NMR spectroscopy. eMagRes. 2007.
53. J. Hu J, Herzfeld J. Baluns, a fine balance and impedance adjustment module, a multi-layer transmission line, and transmission line NMR probes using same. Patent 7936171 B2. 2011.
54. McKay RA. Probes for special purposes. eMagRes. 2007.
55. Schaefer J, McKay RA. Multi-tuned single coil transmission line probe for nuclear magnetic resonance spectrometer. Patent 5861748. 1999.

56. Grant CV, Wu CH, Opella SJ. Probes for high field solid-state NMR of lossy biological samples. J Magn Reson. 2010;204:180–8.
57. Doty FD. Probe design and construction. eMagRes. 2007.
58. Paulson EK, Martin RW, Zilm KW. Cross polarization, radio frequency field homogeneity, and circuit balancing in high field solid state NMR probes. J Magn Reson. 2004;171: 314–23.
59. Becerra LR, Gerfen GJ, Bellew BF, Bryant JA, Hall DA, Inati SJ, Weber RT, Un S, Prisner TF, Mcdermott AE, Fishbein KW, Kreischer KE, Temkin RJ, Singel DJ, Griffin RG. A spectrometer for dynamic nuclear-polarization and electron-paramagnetic-resonance at high- frequencies. J Magn Reson Ser A. 1995;117:28–40.
60. Bajaj VS, Farrar CT, Hornstein MK, Mastovsky I, Vieregg J, Bryant J, Eléna B, Kreischer KE, Temkin RJ, Griffin RG. Dynamic nuclear polarization at 9T using a novel 250 GHz gyrotron microwave source. J Magn Reson. 2003;160:85–90.
61. Pike KJ, Kemp TF, Takahashi H, Day R, Howes AP, Kryukov EV, MacDonald JF, Collis AE, Bolton DR, Wylde RJ, Orwick M, Kosuga K, Clark AJ, Idehara T, Watts A, Smith GM, Newton ME, Dupree R, Smith ME. A spectrometer designed for 6.7 and 14.1 T DNP-enhanced solid-state MAS NMR using quasi-optical microwave transmission. J Magn Reson. 2012;215:1–9.
62. Saliba E, Sesti EL, Scott FJ, Albert BJ, Choi EJ, Alaniva N, Gao C, Barnes AB. Electron decoupling with dynamic nuclear polarization in rotating solids. J Am Chem Soc. 2017;139:6310–3.
63. Hu KN, Bajaj VS, Rosay M, Griffin RG. High-frequency dynamic nuclear polarization using mixtures of TEMPO and trityl radicals. J Chem Phys. 2007;126:044512.
64. Corzilius B, Smith AA, Barnes AB, Luchinat C, Bertini L, Griffin RG. High-field dynamic nuclear polarization with high-spin transition metal ions. J Am Chem Soc. 2011;133:5648–51.
65. Corzilius B, Smith AA, Griffin RG. Solid effect in magic angle spinning dynamic nuclear polarization. J Chem Phys. 2012;137:054201.
66. Smith AA, Corzilius B, Barnes AB, Maly T, Griffin RG. Solid effect dynamic nuclear polarization and polarization pathways. J Chem Phys. 2012;136:015101.
67. Can TV, Ni QZ, Griffin RG. Mechanisms of dynamic nuclear polarization in insulating solids. J Magn Reson. 2015;253:23–35.
68. Lelli M, Chaudhari SR, Gajan D, Casano G, Rossini AJ, Ouari O, Tordo P, Lesage A, Emsley L. Solid-state dynamic nuclear polarization at 9.4 and 18.8 T from 100 K to room temperature. J Am Chem Soc. 2015;137:14558–61.
69. Abragam A, Proctor WG. Une Nouvelle Methode De Polarisation Dynamique Des Noyaux Atomiques Dans Les Solides. Cr Hebd Acad Sci. 1958;246:2253–6.
70. Afeworki M, Schaefer J. Mechanism of DNP-enhanced polarization transfer across the interface of polycarbonate/polystyrene heterogeneous blends. Macromolecules. 1992;25:4092–6.
71. Erb E, Motchane JL, Ubersfeld CR. Acad Sci. 1958;246:2253.
72. Hwang CF, Hill DA. Phenomenological model for new effect in dynamic polarization. Phys Rev Lett. 1967;19:1011.
73. Hwang CF, Hill DA. New effect in dynamic polarization. Phys Rev Lett. 1967;18:110.
74. Jeffries CD. Polarization of nuclei by resonance saturation in paramagnetic crystals. Phys Rev. 1957;106:164–5.
75. Kessenikh AV, Lushchikov VI, Manenkov AA, Taran YV. Proton polarization in irradiated polyethylenes. Sov Phys-Sol State. 1963;5:321–9.
76. Kessenikh AV, Manenkov AA, Pyatnitskii GI. On explanation of experimental data on dynamic polarization of protons in irradiated polyethylenes. Sov Phys Solid State. 1964;6:641–3.
77. Overhauser AW. Polarization of nuclei in metals. Phys Rev. 1953;92:411–5.
78. Wollan DS. Dynamic nuclear-polarization with an inhomogeneously broadened ESR Line. 1. Theory. Phys Rev B. 1976;13:3671–85.

79. Hovav Y, Feintuch A, Vega S. Theoretical aspects of dynamic nuclear polarization in the solid state – the cross effect. J Magn Reson. 2012;214:29–41.
80. Hovav Y, Levinkron O, Feintuch A, Vega S. Theoretical aspects of dynamic nuclear polarization in the solid state: the influence of high radical concentrations on the solid effect and cross effect mechanisms. Appl Magn Reson. 2012;43:21–41.
81. Mentink-Vigier F, Akbey Ü, Hovav Y, Vega S, Oschkinat H, Feintuch A. Fast passage dynamic nuclear polarization on rotating solids. J Magn Reson. 2012;224:13–21.
82. Shimon D, Hovav Y, Feintuch A, Goldfarb D, Vega S. Dynamic nuclear polarization in the solid state: a transition between the cross effect and the solid effect. Phys Chem Chem Phys. 2012;14:5729–43.
83. Hu K-N. Polarizing agents and mechanisms for high-field dynamic nuclear polarization of frozen dielectric solids. Solid State Nucl Magn Reson. 2011;40:31–41.
84. Hu KN, Debelouchina GT, Smith AA, Griffin RG. Quantum mechanical theory of dynamic nuclear polarization in solid dielectrics. J Chem Phys. 2011;134:125105.
85. Hu K-N, Bajaj VS, Rosay M, Griffin RG. High-frequency dynamic nuclear polarization using mixtures of TEMPO and trityl radicals. J Chem Phys. 2007;126:044512.
86. Song CS, Hu KN, Joo CG, Swager TM, Griffin RG. TOTAPOL: a biradical polarizing agent for dynamic nuclear polarization experiments in aqueous media. J Am Chem Soc. 2006;128:11385–90.
87. Michaelis VK, Corzilius B, Smith AA, Griffin RG. Dynamic nuclear polarization of ^{17}O: direct polarization. J Phys Chem B. 2013;117:14894–906.
88. Michaelis VK, Smith AA, Corzilius B, Haze O, Swager TM, Griffin RG. High-field ^{13}C DNP with a radical mixture. J Am Chem Soc. 2013;135:2935–8.
89. Thurber KR, Tycko R. Theory for cross effect dynamic nuclear polarization under magic-angle spinning in solid state nuclear magnetic resonance: the importance of level crossings. J Chem Phys. 2012;137:084508.
90. Jeffries CD. Dynamic orientation of nuclei by forbidden transitions in paramagnetic Resonance. Phys Rev. 1960;117:1056–69.
91. Smith AN, Long JR. Dynamic nuclear polarization as an enabling technology for solid state nuclear magnetic resonance spectroscopy. Anal Chem. 2016;88:122–32.
92. Lafon O, Thankamony ASL, Rosay M, Aussenac F, Lu X, Trebosc J, Bout-Roumazeilles V, Vezin H, Amoureux J-P. Indirect and direct ^{29}Si dynamic nuclear polarization of dispersed nanoparticles. Chem Commun. 2013;49:2864–6.
93. Maly T, Andreas LB, Smith AA, Griffin RG. ^{2}H-DNP-enhanced ^{2}H-^{13}C solid-state NMR correlation spectroscopy. Phys Chem Chem Phys. 2010;12:5872–8.
94. Ardenkjær-Larsen JH, Fridlund B, Gram A, Hansson G, Hansson L, Lerche MH, Servin R, Thaning M, Golman K. Increase in signal-to-noise ratio of $>$ 10,000 times in liquid-state NMR. Proc Natl Acad Sci. 2003;100:10158–63.
95. Dementyev AE, Cory DG, Ramanathan C. High-field overhauser dynamic nuclear polarization in silicon below the metal–insulator transition. J Chem Phys. 2011;134:154511.
96. Hu K-N, Song C, Yu H-h, Swager TM, Griffin RG. High-frequency dynamic nuclear polarization using biradicals: a multifrequency EPR lineshape analysis. J Chem Phys. 2008;128:052302.
97. Ardenkjaer-Larsen JH, Macholl S, Johannesson H. Dynamic nuclear polarization with trityls at 1.2 K. Appl Magn Reson. 2008;34:509–22.
98. Reynolds S, Patel H. Monitoring the solid-state polarization of ^{13}C, ^{5}N, ^{2}H, ^{29}Si and ^{31}P. Appl Magn Reson. 2008;34:495–508.
99. Can TV, Caporini MA, Mentink-Vigier F, Corzilius B, Walish JJ, Rosay M, Maas WE, Baldus M, Vega S, Swager TM, Griffin RG. Overhauser effects in insulating solids. J Chem Phys. 2014;141:064202.
100. Corzilius B, Andreas LB, Smith AA, Ni QZ, Griffin RG. Paramagnet induced signal quenching in MAS–DNP experiments in frozen homogeneous solutions. J Magn Reson. 2014;240:113–23.

101. Mathies G, Caporini MA, Michaelis VK, Liu Y, Hu K-N, Mance D, Zweier JL, Rosay M, Baldus M, Griffin RG. Efficient dynamic nuclear polarization at 800 MHz/527 GHz with trityl- nitroxide biradicals. Angew Chem Int Ed. 2015;54:11770–4.
102. Sauvée C, Casano G, Abel S, Rockenbauer A, Akhmetzyanov D, Karoui H, Siri D, Aussenac F, Maas W, Weber RT, Prisner T, Rosay M, Tordo P, Ouari O. Tailoring of polarizing agents in the bTurea series for cross-effect dynamic nuclear polarization in aqueous media. Chem Eur J. 2016;22:5598–606.
103. Kubicki DJ, Casano G, Schwarzwalder M, Abel S, Sauvee C, Ganesan K, Yulikov M, Rossini AJ, Jeschke G, Coperet C, Lesage A, Tordo P, Ouari O, Emsley L. Rational design of dinitroxide biradicals for efficient cross-effect dynamic nuclear polarization. Chem Sci. 2016;7:550–8.
104. Matsuki Y, Maly T, Ouari O, Karoui H, Le Moigne F, Rizzato E, Lyubenova S, Herzfeld J, Prisner T, Tordo P, Griffin RG. Dynamic nuclear polarization with a rigid biradical. Angew Chem Int Ed. 2009;48:4996–5000.
105. Sauvée C, Rosay M, Casano G, Aussenac F, Weber RT, Ouari O, Tordo P. Highly efficient, water-soluble polarizing agents for dynamic nuclear polarization at high frequency. Angew Chem Int Ed. 2013;52:10858–61.
106. Zagdoun A, Casano G, Ouari O, Schwarzwälder M, Rossini AJ, Aussenac F, Yulikov M, Jeschke G, Copéret C, Lesage A, Tordo P, Emsley L. Large molecular weight nitroxide biradicals providing efficient dynamic nuclear polarization at temperatures up to 200 K. J Am Chem Soc. 2013;135:12790–7.
107. Zagdoun A, Casano G, Ouari O, Lapadula G, Rossini AJ, Lelli M, Baffert M, Gajan D, Veyre L, Maas WE, Rosay M, Weber RT, Thieuleux C, Coperet C, Lesage A, Tordo P, Emsley L. A slowly relaxing rigid biradical for efficient dynamic nuclear polarization surface-enhanced NMR spectroscopy: expeditious characterization of functional group manipulation in hybrid materials. J Am Chem Soc. 2012;134:2284–91.
108. Kiesewetter MK, Corzilius B, Smith AA, Griffin RG, Swager TM. Dynamic nuclear polarization with a water-soluble rigid biradical. J Am Chem Soc. 2012;134:4537–40.
109. Ong TC, Mak-Jurkauskas ML, Walish JJ, Michaelis VK, Corzilius B, Smith AA, Clausen AM, Cheetham JC, Swager TM, Griffin RG. Solvent-free dynamic nuclear polarization of amorphous and crystalline ortho-terphenyl. J Phys Chem B. 2013;117:3040–6.
110. Kiesewetter MK, Michaelis VK, Walish JJ, Griffin RG, Swager TM. High field dynamic nuclear polarization NMR with surfactant sheltered biradicals. J Phys Chem B. 2014;118:1825–30.
111. Dane EL, Corzilius B, Rizzato E, Stocker P, Ouari O, Maly T, Smith AA, Griffin RG, Ouari O, Tordo P, Swager TM. Rigid orthogonal bis-TEMPO biradicals with improved solubility for dynamic nuclear polarization. J Org Chem. 2012;77:1789–97.
112. Kaushik M, Bahrenberg T, Can TV, Caporini MA, Silvers R, Heiliger J, Smith AA, Schwalbe H, Griffin RG, Corzilius B. Gd(III) and Mn(II) complexes for dynamic nuclear polarization: small molecular chelate polarizing agents and applications with site-directed spin labeling of proteins. Phys Chem Chem Phys. 2016;18:27205–18.
113. Corzilius B. Theory of solid effect and cross effect dynamic nuclear polarization with half-integer high- spin metal polarizing agents in rotating solids. Phys Chem Chem Phys. 2016;18:27190–204.
114. Wenk P, Kaushik M, Richter D, Vogel M, Suess B, Corzilius B. Dynamic nuclear polarization of nucleic acid with endogenously bound manganese. J Biomol NMR. 2015;63:97–109.
115. Corzilius B, Michaelis VK, Penzel S, Ravera E, Smith AA, Luchinat C, Griffin RG. Dynamic nuclear polarization of ^{1}H, ^{l3}C, and ^{59}Co in a Tris(ethylenediamine)cobalt(III) crystalline lattice doped with Cr(III). J Am Chem Soc. 2014;136:11716–27.
116. Hall DA, Maus DC, Gerfen GJ, Inati SJ, Becerra LR, Dahlquist FW, Griffin RG. Polarized-enhanced NMR spectroscopy of biomolecules in frozen solution. Science. 1997;276:930–2.
117. Eaton GR, Eaton SS, Barr DP, Weber RT. Quantitative EPR. New York: SpringerWien; 2010.

118. Wada T, Yamanaka M, Fujihara T, Miyazato Y, Tanaka K. Experimental and theoretical evaluation of the charge distribution over the ruthenium and dioxolene framework of [Ru (OAc)(dioxolene)(terpy)] (terpy = 2,2‘:6‘,2“-terpyridine) depending on the substituents. Inorg Chem. 2006;45:8887–94.
119. Zagdoun A, Rossini AJ, Gajan D, Bourdolle A, Ouari O, Rosay M, Maas WE, Tordo P, Lelli M, Emsley L, Lesage A, Coperet C. Non-aqueous solvents for DNP surface enhanced NMR spectroscopy. Chem Commun. 2012;48:654–6.
120. Liao SY, Lee M, Wang T, Sergeyev IV, Hong M. Efficient DNP NMR of membrane proteins: sample preparation protocols, sensitivity, and radical location. J Biomol NMR. 2016;64:223–37.
121. Debelouchina GT, Bayro MJ, Van der Wel PCA, Caporini MA, Barnes AB, Rosay M, Maas WE, Griffin RG. Dynamic nuclear polarization-enhanced solid-state NMR spectroscopy of GNNQQNY nanocrystals and amyloid fibrils. Phys Chem Chem Phys. 2010;12:5911–9.
122. Gunther WR, Michaelis VK, Caporini MA, Griffin RG, Román-Leshkov Y. Dynamic nuclear polarization NMR enables the analysis of Sn-beta zeolite prepared with natural abundance ^{119}Sn precursors. J Am Chem Soc. 2014;136:6219–22.
123. Van der Wel PCA, Hu KN, Lewandowski J, Griffin RG. Dynamic nuclear polarization of amyloidogenic peptide nanocrystals: GNNQQNY, a core segment of the yeast prion protein Sup35p. J Am Chem Soc. 2006;128:10840–6.
124. Lange S, Linden AH, Akbey Ü, Trent Franks W, Loening NM, van Rossum B-J, Oschkinat H. The effect of biradical concentration on the performance of DNP-MAS-NMR. J Magn Reson. 2012;216:209–12.
125. Rossini AJ, Zagdoun A, Hegner F, Schwarzwälder M, Gajan D, Copéret C, Lesage A, Emsley L. Dynamic nuclear polarization NMR spectroscopy of microcrystalline solids. J Am Chem Soc. 2012;134:16899–908.
126. Rossini AJ, Zagdoun A, Lelli M, Canivet J, Aguado S, Ouari O, Tordo P, Rosay M, Maas WE, Copéret C, Farrusseng D, Emsley L, Lesage A. Dynamic nuclear polarization enhanced solid-state NMR spectroscopy of functionalized metal–organic frameworks. Angew Chem Int Ed. 2012;51:123–7.
127. Mak-Jurkauskas ML, Bajaj VS, Hornstein MK, Belenky M, Griffin RG, Herzfeld J. Energy transformations early in the bacteriorhodopsin photocycle revealed by DNP-enhanced solid-state NMR. Proc Natl Acad Sci U S A. 2008;105:883–8.
128. Bajaj VS, Mak-Jurkauskas ML, Belenky M, Herzfeld J, Griffin RG. Functional and shunt states of bacteriorhodopsin resolved by 250 GHz dynamic nuclear polarization-enhanced solid-state NMR. Proc Natl Acad Sci U S A. 2009;106:9244–9.
129. Barnes AB, Corzilius B, Mak-Jurkauskas ML, Andreas LB, Bajaj VS, Matsuki Y, Belenky ML, Lugtenburg J, Sirigiri JR, Temkin RJ, Herzfeld J, Griffin RG. Resolution and polarization distribution in cryogenic DNP/MAS experiments. Phys Chem Chem Phys. 2010;12:5861–7.
130. Voinov MA, Good DB, Ward ME, Milikisiyants S, Marek A, Caporini MA, Rosay M, Munro RA, Ljumovic M, Brown LS, Ladizhansky V, Smirnov AI. Cysteine-specific labeling of proteins with a nitroxide biradical for dynamic nuclear polarization NMR. J Phys Chem B. 2015;119:10180–90.
131. Wylie BJ, Dzikovski BG, Pawsey S, Caporini M, Rosay M, Freed JH, McDermott AE. Dynamic nuclear polarization of membrane proteins: covalently bound spin-labels at protein–protein interfaces. J Biomol NMR. 2015;61:361–7.
132. Andreas LB, Barnes AB, Corzilius B, Chou JJ, Miller EA, Caporini M, Rosay M, Griffin RG. Dynamic nuclear polarization study of inhibitor binding to the M2 proton transporter from influenza A. Biochemistry. 2013;52:2774–82.
133. Bayro MJ, Debelouchina GT, Eddy MT, Birkett NR, MacPhee CE, Rosay M, Maas WE, Dobson CM, Griffin RG. Intermolecular structure determination of amyloid fibrils with magic-angle spinning, dynamic nuclear polarization NMR. J Am Chem Soc. 2011;133:13967–74.
134. Bayro MJ, Maly T, Birkett N, MacPhee C, Dobson CM, Griffin RG. High-resolution MAS NMR analysis of PI3-SH3 amyloid fibrils: backbone conformation and implications for protofilament assembly and structure. Biochemistry. 2010;49:7474–88.

135. Debelouchina GT, Platt GW, Bayro MJ, Radford SE, Griffin RG. Intermolecular alignment in β 2-microglobulin amyloid fibrils. J Am Chem Soc. 2010;132:17077–9.
136. Rossini AJ, Zagdoun A, Hegner F, Schwarzwälder M, Gajan D, Coperet C, Lesage A, Emsley L. Dynamic nuclear polarization NMR spectroscopy of microcrystalline solids. J Amer Chem Soc. 2012;134:16899–908.
137. Lesage A, Lelli M, Gajan D, Caporini MA, Vitzthum V, Mieville P, Alauzun J, Roussey A, Thieuleux C, Mehdi A, Bodenhausen G, Copéret C, Emsley L. Surface enhanced NMR spectroscopy by dynamic nuclear polarization. J Am Chem Soc. 2010;132:15459–61.
138. Debelouchina GT, Bayro MJ, van der Wel PCA, Caporini MA, Barnes AB, Rosay M, Maas WE, Griffin RG. Dynamic nuclear polarization-enhanced solid-state NMR spectroscopy of GNNQQNY nanocrystals and amyloid fibrils. Phys Chem Chem Phys. 2010;12:5911–9.
139. Lelli M, Gajan D, Lesage A, Caporini MA, Vitzthum V, Mieville P, Heroguel F, Rascon F, Roussey A, Thieuleux C, Boualleg M, Veyre L, Bodenhausen G, Copéret C, Emsley L. Fast characterization of functionalized silica materials by silicon-29 surface-enhanced NMR spectroscopy using dynamic nuclear polarization. J Am Chem Soc. 2011;133:2104–7.
140. Frederick KK, Michaelis VK, Corzilius B, Ong T-C, Jacavone AC, Griffin RG, Lindquist S. Sensitivity-enhanced NMR reveals alterations in protein structure by cellular milieus. Cell. 2015;163:620–8.
141. Lafon O, Thankamony ASL, Kobayashi T, Carnevale D, Vitzthum V, Slowing II, Kandel K, Vezin H, Amoureux J-P, Bodenhausen G, Pruski M. Mesoporous silica nanoparticles loaded with surfactant: low temperature magic angle spinning ^{13}C and ^{29}Si NMR enhanced by dynamic nuclear polarization. J Phys Chem C. 2013;117:1375–82.
142. Lee D, Duong NT, Lafon O, De Paëpe G. Primostrato solid-state NMR enhanced by dynamic nuclear polarization: pentacoordinated Al^{3+} ions are only located at the surface of hydrated γ – alumina. J Phys Chem C. 2014;118:25065–76.
143. Takahashi H, Ayala I, Bardet M, De Paëpe G, Simorre J-P, Hediger S. Solid-state NMR on bacterial cells: selective cell wall signal enhancement and resolution improvement using dynamic nuclear polarization. J Am Chem Soc. 2013;135:5105–10.
144. Takahashi H, Hediger S, De Paëpe G. Matrix-free dynamic nuclear polarization enables solid-state NMR ^{13}C- ^{13}C correlation spectroscopy of proteins at natural isotopic abundance. Chem Commun. 2013;49:9479–81.
145. Thankamony ASL, Lafon O, Lu X, Aussenac F, Rosay M, Trébosc J, Vezin H, Amoureux J-P. Solvent-free high-field dynamic nuclear polarization of mesoporous silica functionalized with TEMPO. Appl Magn Reson. 2012;43:237–50.
146. Ravera E, Corzilius B, Michaelis VK, Rosa C, Griffin RG, Luchinat C, Bertini I. Dynamic nuclear polarization of sedimented solutes. J Am Chem Soc. 2013;134:1641–4.
147. Ravera E, Corzilius B, Michaelis VK, Luchinat C, Griffin RG, Bertini I. DNP-enhanced MAS NMR of bovine serum albumin sediments and solutions. J Phys Chem B. 2014;118:1825–30.
148. Smith AN, Caporini MA, Fanucci GE, Long JR. A method for dynamic nuclear polarization enhancement of membrane proteins. Angew Chem Int Ed. 2015;54:1542–6.